

# Powered Super Tail: A Terrain-Adaptive Wheel-legged Robotic Limb to Assist Human's Load Carriage

Yanzhen Xiang, Xiaoyu Yan<sup>#</sup>, Hanqi Su<sup>#</sup>, Nuo Chen<sup>#</sup>, Shangkun Guo, Jielin Wu, Yuquan Leng<sup>\*</sup> and Chenglong Fu<sup>\*</sup>

**Abstract**— Load carriage is a common demand in humans' daily life. Long time load carriage often causes significant energy expenditure for the body and may even bring physical problems like muscle strain. Variations in terrains and ground conditions are usually inevitable in such scenarios, which disrupts humans' gait and leads to even more energy expenditure. In this paper, a wheel-legged robotic limb, Powered Super Tail (PST) to assist human's load carriage in varying terrains and ground conditions is proposed. The PST system mainly consists of a support rod transferring load to the ground and a pair of stepping triple wheel groups adaptable to different terrain conditions including ground barriers, stairs and rough roads. Driven by a pair of motors, uplifting support for the load and appropriate force assistance could be effectively provided by the support rod, and thus energy expenditure of human body could be reduced. The system's performance on human body was tested. It is shown that the stepping triple wheel group could successfully traverse barriers of different heights and ascend stairs. The effect of the system on human body standing and walking on flat ground were respectively evaluated under three experimental conditions including 1) with the load only (LOAD, 26.42 kg); 2) with the powered PST (PST\_ON, 37.30 kg); 3) with unpowered PST (PST\_OFF, 37.30 kg). And the percentage of metabolic power consumption reduction was the metric for evaluation. Experiments demonstrate the following results: during standing, the metabolic power consumption under PST\_ON is lowered by 5.42% compared to LOAD and 12.56% compared to PST\_OFF; and during walking, the metabolic power consumption is lowered by 20.85% compared to LOAD and 36.58% compared to PST\_OFF.

**Indexing Terms**— Wearable Robotics, Human Performance Augmentation, Human-Robot Collaboration

## I. INTRODUCTION

Load carriage is a universal need in humans' daily activities. Energy expenditure of human bodies caused by the load is often relatively large, affecting adversely their locomotion ability. For the elderly with relatively poor physical conditions, heavy loads may also cause damage to their physiological functions. For personnel like load delivery

expressman and firefighters, heavy loads make it hard for them to walk or run fast for long, and thus significantly limiting their working efficiency. Additionally, humans often traverse real-world environments with a variety of surface irregularities and inconsistencies, which can disrupt steady gait and require additional effort [1]. These environments may include varying terrains and ground conditions such as ground with barriers, stairs and rough roads.

There are various load carriage assistive systems. Elastically suspended backpacks lower energy consumption of human body by optimizing distribution of load force [2]-[9], but they are only effective in rhythmical motion of human body. Legged exoskeletons support the load and transfer its weight to the ground, thus increasing users' load capacity [10]-[12]. Nevertheless, since their rigid structures are fixed and parallel with human's leg, their inertia and joints are prone to interfere with the user's natural walking and may cause extra biological energy expenditure for the human body [17]. Soft-suit exoskeletons could reduce energy consumption of human bodies in load carriage by applying assistive torques to the joints [13]-[16], but they usually could not effectively provide support for the load due to lack of rigid structure. Recently, novel wearable robots such as Supernumerary Robotic Limb (SRL) and Wheel-legged Robotic Limb (WRL) aiming at saving humans' energy expenditure in load carriage are proposed, whose structures are kinematically independent from humans' legs and could avoid interference with humans' intrinsic motion [18]-[23]. Locomotion-assistive SRL is usually modeled on humans' lower extremity and could adapt to various kinds of terrains. However, its mechanical structure is often relatively complex, which substantially increases energy cost of actuators, limits its maximum speed and makes it technically challenging to be controlled in locomotion. WRL serves as a remedy for these problems. In [23], Yuquan Leng *et. al.* proposed a light weight WRL system using a rigid rod to provide active supporting force for the load. It is relatively easy to be controlled and could adjust to a wide range of locomotion speeds, but at present it still has lots of

This work was supported by the National Natural Science Foundation of China [Grant U1913205 and 51805237]; the National Key R&D Program of China [Grant 2018YFB1305400]; Guangdong Basic and Applied Basic Research Foundation [Grant 2020B1515120098]; Guangdong Innovative and Entrepreneurial Research Team Program [Grant 2016ZT06G587]; Shenzhen and Hong Kong Innovation Circle Project [Grant SGLH20180619172011638]; Joint Fund of Science & Technology Department of Liaoning Province and State Key Laboratory of Robotics, China [Grant No.2020-KF-22-03]; and Centers for Mechanical Engineering Research and Education at MIT and SUSTech. (*Corresponding author: Chenglong Fu, Yuquan Leng*).

Yanzhen Xiang, Xiaoyu Yan, Nuo Chen, Hanqi Su, Shangkun Guo, Jielin Wu, Yuquan Leng and Chenglong Fu are with the Shenzhen Key Laboratory of Biomimetic Robotics and Intelligent Systems and Guangdong Provincial Key Laboratory of Human-Augmentation and Rehabilitation Robotics in Universities, Southern University of Science and Technology, Shenzhen 518055, China, and also with the Department of Mechanical and Energy Engineering, Southern University of Science and Technology, Shenzhen 518055, China. (e-mail: 11811417@mail.sustech.edu.cn; lengyq@sustech.edu.cn; fcul@sustech.edu.cn)

<sup>#</sup>Xiao Yuyan, Hanqi Su and Nuo Chen contributed equally to this work.

<sup>\*</sup>Corresponding authors.

drawbacks. Specifically, the ability of adapting to complicated and unstructured terrains is significantly limited. And force assistance during locomotion is limited to vertical direction.

This paper proposes a new type of WRL system named Powered Super Tail (PST), which could provide not only load support but also force assistance during locomotion in varying terrains and ground conditions. As shown in Figure 1, in the PST system there is a rigid rod supporting the load and transferring its weight to the ground. The rod is connected to the load through a 1-DoF passive rotary joint. Two groups of wheels are at the end of the supporting rod, located at its two sides and symmetrical about the sagittal plane of the human body wearing this system. Each group contains three wheels forming a triangular configuration. Such wheeled mechanism is named stepping triple wheel group, since the triangular configuration formed by its three wheels permits stepping through stairs and obstacles. The wheels are actuated by a pair of motors (two active rotary joints). Adaptive PD control strategy is applied to ensure effective support of the rod during locomotion. To verify adaptation to different terrains of the stepping triple wheel group, tests of traversing barriers and ascending stairs were conducted. And to evaluate the effect of the PST system on human body, a series of experiments were carried out on the treadmill, including measuring and evaluating metabolic power consumption of subjects during standing and walking at 0.8 m/s. The experimental results verify effectiveness of the PST system. In the followings, Section II illustrates the design of the PST system. Section III describes experimental setup and results. And Section IV presents conclusions and discussions.

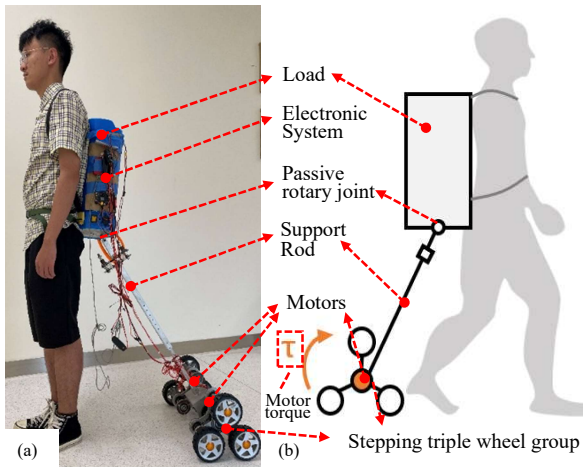


Figure 1. (a) The picture of the PST system worn by the user. (b) The kinematic scheme of the PST system.

## II. SYSTEM DESIGN

During locomotion, the PST system is expected to provide continuous load support and force assistance for the human body, irrespective of speed and terrain conditions. Therefore, the actuators are supposed to continuously output required torque under different operation speeds, and the ground contact mechanism should be adaptive to a wide range of speeds and terrains. Detailed designs according to these requirements are presented in the followings.

### A. Mechanical & Electronical Design

As shown in Figure 2, the PST system mainly consists of three parts: support rod, stepping triple wheel group and electronic system.

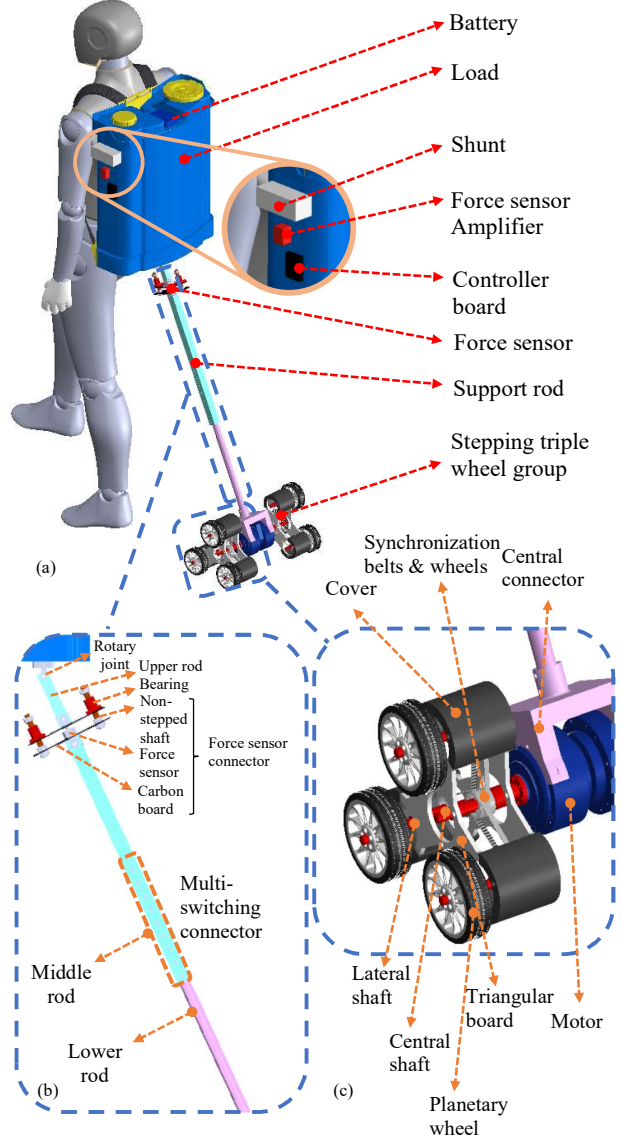


Figure 2. An overview of mechanical and electronical design of the PST system. (b) Detailed design of the support rod. (c) Detailed design of the stepping triple wheel group.

The support rod is composed of several sections. The upper rod is a square rod directly connected with the load through a passive rotary joint. Between the upper rod and the middle rod is the force sensor connector, which contains a force sensor, two pieces of carbon plates, two bearings and two non-stepped shafts. This permits relative slide between parts below and above the force sensor connector. Each non-stepped is tapped at its two ends to install nuts, which limit the range of slides. Such design ensures force component vertical to the rod born by the non-stepped shafts instead of the force sensor, thus preventing the force sensor from being damaged by excessive transverse tension. Below the force se-

nsor connector are the middle and lower rod, and part of the latter is inside the former. The middle rod is square, and the lower rod is cylindrical. The multi-switching connection of these two rods allows adjustment of support rod length. At present, this length is manually selected according to the user's height. Below the lower rod the stepping triple wheel group is connected through a fixed joint.

Here are design parameters and material selection for the support rod. The three mechanical rods are made of aluminum alloy. The upper rod is 100 mm in longitudinal length, 20 mm in outer side length and 2 mm in thickness. And the middle rod is 460 mm in longitudinal length, 25 mm in outer side length and 2 mm in thickness respectively. The lower rod is 520 mm in longitudinal length, 20 mm in outer radius and 2 mm in thickness respectively. Based on the multi-switching design, the length of the supporting rod could be  $855 + 25n$  ( $n = 0, 1, \dots, 9$ ) mm. As for the force sensor connector, the two boards are made of carbon fiber, and the two non-stepping shafts are made of stainless steel. When the user wears the PST system, the moderate tilt angle of the supporting leg is about  $30^\circ$ , which ensures that the support rod could play effective role on the user while avoiding interference with the user's feet.

The stepping triple wheel group contains one sun pivot in the center and three planetary wheels arranged circularly around. Lines connecting centers of sun pivot and planet wheels form  $120^\circ$  angle with their adjacent ones.

The detailed design of the stepping triple wheel group is illustrated as follows. Two pairs of wheels are symmetric about the support rod, and the symmetry axis is in the sagittal plane of the human body. The central connector fixes the support rod, and both of the two sides of the stepping triple wheel group, under which two motors are installed. Each motor connects a central shaft, which serves as the sun pivots of the wheels. Two triangular boards are mounted on each of the central shafts with bearings, and three lateral shafts are uniformly mounted around on the boards. Three synchronization belts connect the central and lateral shafts, which could transfer motions and torques from the sun pivot to planetary wheels. Three wheels are mounted at the end of each lateral shaft.

Here are the design parameters and material selection for the stepping triple wheel group. Most of the components are made of aluminum alloy. The covers are made of resin, and the tires are made of rubber. The radius of planetary wheels is all 62.5 mm. The distances between the sun pivot and centers of the planet wheels are 85.5 mm. The motors are 49.5 mm in radius and 820 g in weight.

The electronic system is mainly composed of the master board, the battery, the force sensor, the force sensor amplifier and two motors. The master board is STM32F427IHX, which controls motions of the motors according to feedback from the force sensor. The 25.2 V battery provide power supply for the whole electronic system through an electric wire, which is divided into several branches through a shunt. The force sensor (LCM 300, Futek, USA) measures the support force of the rod, and the results are amplified by the force sensor amplifier. The motors (AK10-9) outputs a certain torque driving the system forward. Their motions could be controlled

controlled by the master board through CAN communication.

### B. Control System

During load carriage, walking and running are two common cases. Appropriate control strategies should be applied to assure that the support rod could provide effective support during both walking and running. In this scenario, PD force control is applied. The output torques of the motors adjust according to the speed of the human body so that the humans' motion could be tracked in real time.

The block diagram of the control system is shown in Figure 3. Desired support force along the rod is set, and real support force along the rod is measured by the force sensor. Difference between the desired and real force is calculated and input into the PD controller. This controller computes the desired motor torque increment. The desired motor torque is calculated by first integrating desired motor torque increments obtained in the past loops and then goes through an amplitude limiting unit, which limits the torque into a certain range. The main purpose of the amplitude limiting unit is to prevent possible dangers to the user caused by exceedingly large motor torques.

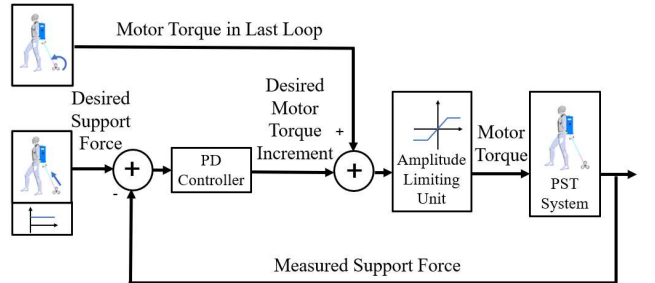


Figure 3. The diagram of the control system of the PST system.

The calculations above can be articulated by the following equations. And meanings of notations are listed in Table 1.

$$\delta\tau_M = k_p \Delta F + k_d \Delta F' \quad (1)$$

$$\Delta F = F_d - F_r \quad (2)$$

$$\tau_M = \begin{cases} \tau_{M,max}, & \int \delta\tau_M > \tau_{M,max} \\ \int \delta\tau_M, & \tau_{M,min} \leq \int \delta\tau_M \leq \tau_{M,max} \\ \tau_{M,min}, & \int \delta\tau_M < \tau_{M,min} \end{cases} \quad (3)$$

Notations	Meanings
$F_d$	Desired support force along the rod
$F_r$	Measured support force along the rod
$\Delta F$	Difference between desired and measured support force
$\delta\tau_M$	Motor torque increment
$\tau_M$	Motor torque
$\tau_{M,max}$	Maximum motor torque
$\tau_{M,min}$	Minimum motor torque

Table 1. Meanings of notations in the equations.

In our experiments, the desired force  $F_d$  is set to 120 N.  $\tau_{M,max}$  and  $\tau_{M,min}$  are set to 1.8 N·m and -1.8 N·m respectively.

tively. Through trials and errors,  $k_p = 0.002$ ,  $k_d = -0.0015$  is found to be an appropriate set of parameters, which could ensure effective support during both walking and standing. The support force and motor torque in experiments is shown in section III.

### III. EXPERIMENTS

#### A. Barrier Stepping Capability of the Stepping Triple Wheel group

Compared to normal wheels, stepping triple wheel group could adapt to various complicated terrains and ground conditions. Here we use the case of traversing barriers and ascending stairs to exemplify this. The wheels group revolves and translates simultaneously. The axis of revolution coincides with the central axis of the planetary wheel contacting ground. When traversing barriers, the order of the planetary wheels remains unchanged after stepping if the barrier is low, as shown in Figure 4 (a). And the planetary wheels change their order if the barrier is high. The ground-contact wheel is wheel A before stepping but wheel C after stepping, as shown in Figure 4 (b). When ascending stairs, each wheel takes turn to be the ground-contact one every three steps. Figure 4 (c) illustrates one step of stair ascending.

Figure 5 illustrates tests of barrier traversing conducted on the prototype of the PST system. The barrier is 50 mm in height. Figure 6 illustrates tests of stair ascending. The stair is 155 mm in height. Each riser of the stairs is 153 mm in height and 300 mm in the distance between each step of the stairs. It is shown that the wheels managed to traverse the barrier being obstructed. The wheels revolved around central axis of the ground-contacting planetary wheel in both tests.

Figure 5 illustrates tests of barrier traversing conducted on the prototype of the PST system. The barrier is 50 mm in height. Figure 6 illustrates tests of stair ascending. The stair is 155 mm in height. Each riser of the stairs is 153 mm in height and 300 mm in the distance between each step of the stairs. It is shown that the wheels managed to traverse the barrier being obstructed. The wheels revolved around central axis of the ground-contacting planetary wheel in both tests.

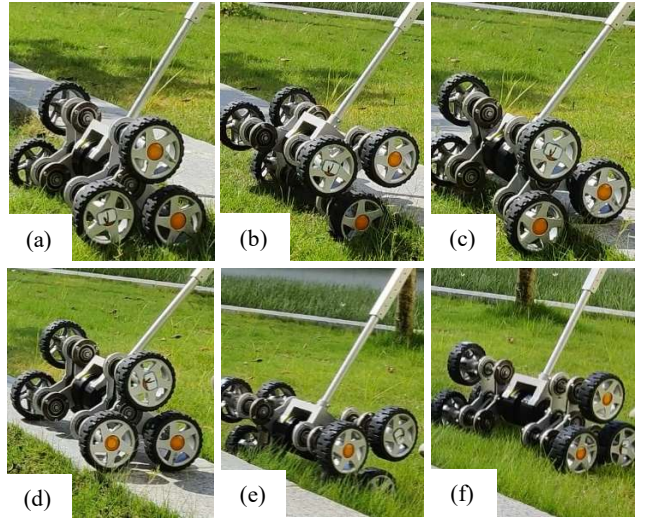


Figure 5. Pictures of the wheels stepping through a barrier. (a)-(c) The wheels step up the barrier. (d)-(f) The wheels step down the barrier.

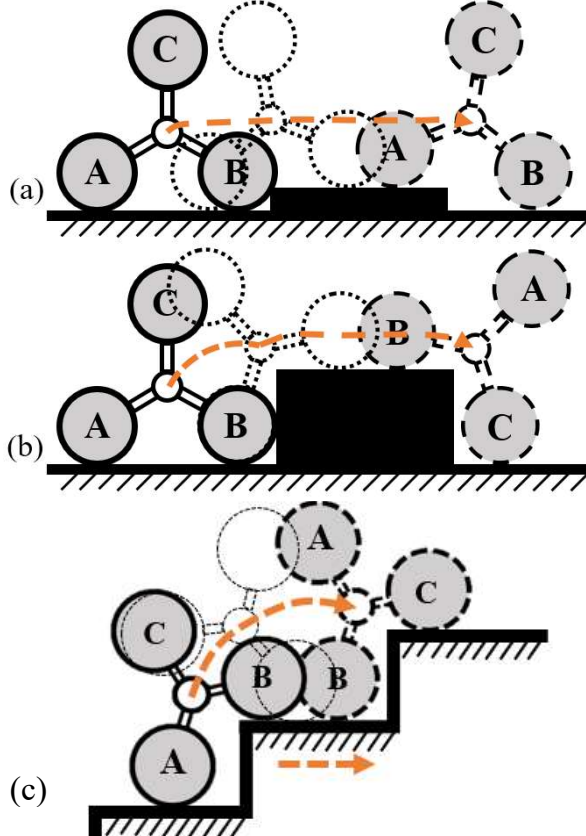


Figure 4. The diagrams of barrier traversing and stair ascending of the wheels. (a) The order of the planetary wheels remains the same after stepping if the barrier is low. (b) The order of the planetary wheels changes after stepping if the barrier is high. (c) One step of stair ascending. B takes the place of A to become the ground-contact wheel after ascending one step.

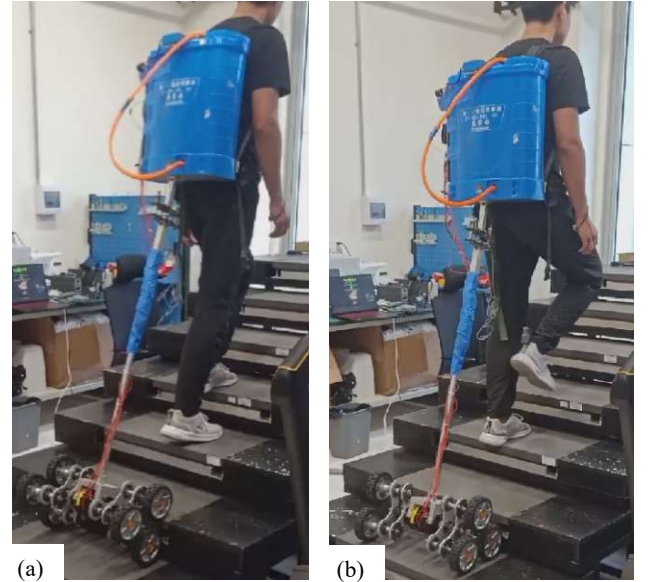


Figure 6. Pictures of the PST system climbing up stairs. (a) The wheels are revolving and climbing one riser. (b) The wheels have climbed up one riser.

#### B . Experiments of the System's Assistance Performance on Flat-Ground Standing and Walking

The subjects selected for tests are three young men  $72.7 \pm 2.52$  kg in weight,  $175.3 \pm 4.99$  cm in height and aging  $20.97 \pm 0.09$  years old. As shown in Figure 7, the tests were conducted on a treadmill (FIT, Bertec, USA). The subjects had obtained informed consent before the experiment. The experiments were carried out in the Human Augmentation



Figure 7. Experimental methods. (a)-(c) Three experiment groups (PST\_ON, PST\_OFF, LOAD) during standing. (d)-(f) Three experiment groups (PST\_ON, PST\_OFF, LOAD) during walking.

Robot Laboratory at Southern University of Science and Technology. The work had been approved by ethical committees where it was performed.

To evaluate the effectiveness of the PST system, we measured the metabolic power consumption of the subject during both standing and walking at 0.8 m/s using a portable indirect calorimetry system (K5, COSMED, Italy, Accuracy:  $1 \times 10^{-7}$  mL/min). In each case, the experiments were divided into three groups: one treatment group and two control groups. The experimental condition of the treatment group is PST\_ON: wearing the PST system with motors powered on and in normal operation. The experimental conditions of control groups are PST\_OFF: wearing the whole PST system with motors unpowered during walking and standing, and LOAD: only carrying the load without other components of the system. The results of PST\_OFF group were compared with those of PST\_ON group to find how significant effect of enhancing performance of a purely passive PST system could the actuators have. And the results of LOAD group were compared with those of PST\_ON group to find how significant effect of an active PST system in saving the energy consumption compared with normal loaded standing or walking. The experimental scheme is to have the subject stand and walk on a treadmill for 8 minutes at a constant speed of 0.8 m/s. The subject rests for 10 minutes after each group is completed during the walking experiment. The results are based on the mean value of measured metabolic power consumption normalized the subject's mass (W/kg) in the last 3 minutes of each experiment.

The support force along the rod and expected torques of the motors during standing and walking in one gait cycle are illustrated in Figure 8. During standing and walking, the rod could provide support in both the PST\_ON and PST\_OFF condition, but effect of the latter is much less significant than that of the former, especially during walking. This is because the rod could transfer load to the ground without driven by motors, but the effect is quite limited, since the rod is inclined in an angle of 30 degrees or so with the vertical direction. During walking in PST\_OFF condition, the motion of the stepping triple wheel group tends to lag the human body due to their inertial and friction with the ground, which further reduces the support force. The figure also shows that the force of support periodically fluctuates in one gait cycle during walking (solid green line), and the motor torque also adjusts according to the force (dotted yellow line). When the support

force increases, the motor torque decreases to lower the excessive support, and then the support force decreases consequently. Vice versa.

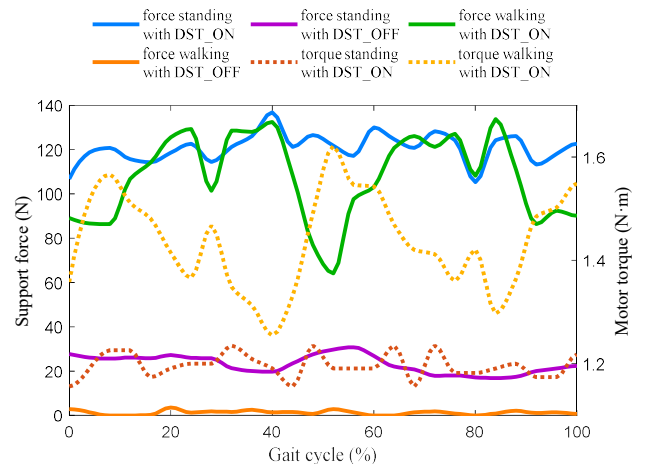


Figure 8. The support force along the rod and the torque of the motors in a gait cycle.

The mean values of metabolic power consumption of the three subjects during standing and walking are respectively presented in Figure 9. During standing, the metabolic power consumption in PST\_ON condition was reduced by 5.42% compared to the LOAD condition and 12.56% compared to the PST\_OFF condition. This indicates that the PST system could effectively reduce the energy consumption of a subject standing still in PST\_ON condition. And during walking, the metabolic power consumption in PST\_ON condition was re-

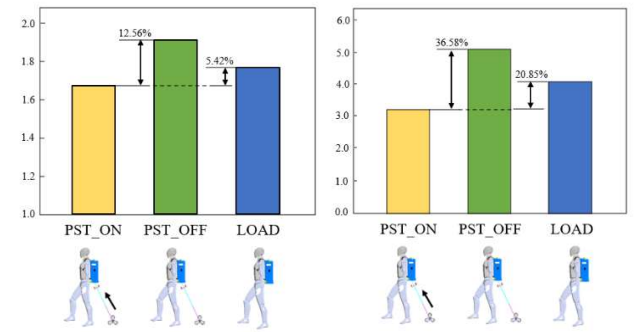


Figure 9. The metabolic power consumption during (a) standing (b) walking, both respectively in PST\_ON, PST\_OFF and LOAD conditions.

duced by 36.58% compared to PST\_OFF condition and 20.85% compared to LOAD condition. This indicates that the PST system could save energy consumption of the walking in 0.8 m/s in PST\_ON condition. In PST\_OFF condition, the energy consumption is even much higher than the normal loaded walking and this is because the motion of the inertia of the wheels causes much more body energy expenditure.

#### IV. CONCLUSIONS AND DISCUSSIONS

In this paper, a novel WRL system named Powered Super Tail (PST for short) aiming at providing load support and force assistance for individuals during load carriage in different terrains and ground conditions is presented. The performances of the system on human body during standing and walking at 0.8 m/s were respectively evaluated. In the experiments, the targeting support force of the rod was set to 110 N. And collected data of the support rod force shows that the support force could keep around the expected value during standing and fluctuate around the expected value during walking. Results demonstrate that the system could lower metabolic power consumption by 12.56% and 5.42% during standing, and 36.58% and 20.85% during walking compared to the condition of PST\_OFF and LOAD. These results all serve as proofs of the system's effects.

There are several aspects to be further improved in the future. For example, experiments can be more comprehensive in testing the system's performance in different speeds of walking and different terrains. Mechanical structures and control strategies can also be optimized to make the system more effective in different terrains like stairs. And combined with other wearable robots like exoskeletons and elastic backpack, the system may play a more significant role, and other novel solutions may also emerge. In brief, the PST system sheds light on the design of assistive systems for load carriage in different terrains and could possibly be combined with other wearable robots to play a more significant role in assistance.

#### ACKNOWLEDGMENT

The authors would like to thank all participants in the experiments. Our deepest gratitude goes to the editor and anonymous reviewers for their careful work and thoughtful suggestions that have helped improve this paper substantially.

#### REFERENCES

- [1] D. B. Kowalsky, J. R. Rebula, L. V. Ojeda, P. G. Adamczyk, and A. D. Kuo, "Human walking in the real world: Interactions between terrain type, gait parameters, and energy expenditure," *PLoS One*, vol. 16, no. 1, p. e0228682, 2021.
- [2] D. Li, T. Li, Q. Li, T. Liu, J. Yi, "A simple model for predicting walking energetics with elastically-suspended backpack," *Journal of Biomechanics*, vol. 49, no. 16, pp. 4150-4153, 2016.
- [3] Y. Wu, K. Chen, C. Fu, "Effects of load connection form on efficiency and kinetics of biped walking," *Journal of Mechanisms and Robotics*, vol. 8, no. 6, pp. 061015, 2016.
- [4] L. Yang, J. Zhang, Y. Xu, K. Chen, and C. Fu, "Energy performance analysis of a suspended backpack with an optimally controlled variable damper for human load carriage," *Mechanism and Machine Theory*, vol. 146, pp. 103738, 2020.
- [5] Y. Leng, X. Lin, Z. Lu, A. Song, Z. Yu, and C. Fu, "A model to predict ground reaction force for elastically-suspended backpacks," *Gait & Posture*, vol. 82, pp. 118-125, 2020.
- [6] Y. Leng, X. Lin, L. Yang, Y. Xu, and C. Fu, "Design of an elastically suspended backpack with tunable stiffness," *In 2020 5th International Conference on Advanced Robotics and Mechatronics (ICARM)*, 2020, pp. 359-363.
- [7] L. Yang, Y. Xu, K. Zhang, K. Chen and C. Fu, "Allowing the Load to Swing Reduces the Mechanical Energy of the Stance Leg and Improves the Lateral Stability of Human Walking," *IEEE Transactions on Neural Systems and Rehabilitation Engineering*, vol. 29, pp. 429-441, 2021.
- [8] L. He, C. Xiong, Q. Zhang, W. Chen, C. Fu, and K. Lee, "A Backpack Minimizing the Vertical Acceleration of the Load Improves the Economy of Human Walking," *IEEE Transactions on Neural Systems and Rehabilitation Engineering*, vol. 28, no. 9, pp. 1994-2004, 2020.
- [9] L. Yang, Y. Xu, J. Zhang, K. Chen, and C. Fu, "Design of an Elastically Suspended Backpack with a Tunable Damper," *2019 IEEE International Conference on Advanced Robotics and its Social Impacts (ARSO)*, 2019, pp. 180-185.
- [10] C. J. Walsh, K. Endo, and H. Herr, "A Quasipassive leg exoskeleton for load-carrying augmentation," *International Journal of Humanoid Robotics*, vol. 4, no. 3, pp. 487-506, 2007.
- [11] Zoss, A. B., Kazerooni, H., and Chu, A., "Biomechanical Design of the Berkeley Lower Extremity Exoskeleton (BLEEX)". *IEEE/ASME Transactions on Mechatronics*, 11(2), pp. 128–138, 2006.
- [12] Kazerooni, H., Steger, R., and Huang, L., "Hybrid Control of the Berkeley Lower Extremity Exoskeleton (BLEEX)". *The International Journal of Robotics Research*, 25(5-6), pp. 561–573, 2006.
- [13] L. M. Mooney, E. J. Rouse, and H. M. Herr, "Autonomous exoskeleton reduces metabolic cost of human walking during load carriage," *Journal of Neuroengineering and Rehabilitation*, vol. 11, no.1, pp. 1-11, 2014.
- [14] L. M. Mooney, and H. M. Herr, "Biomechanical walking mechanisms underlying the metabolic reduction caused by an autonomous exoskeleton," *Journal of Neuroengineering and Rehabilitation*, vol.13, no.4, pp. 1-12, 2016.
- [15] J. Liu, C. Xiong, and C. Fu, "An ankle exoskeleton using a lightweight motor to create high power assistance for push-off," *Journal of Mechanisms and Robotics-Transactions of the ASME*, vol. 11, no.4, pp. 041001, 2019.
- [16] F. A. Panizzolo, I. Galiana, A. T. Asbeck, C. Siviy, K. Schmidt, K. G. Holt, and C. J. Walsh, "A Biologically-inspired Multi-joint Soft Exosuit that Can Reduce the Energy Cost of Loaded Walking". *Journal of Neuroengineering and Rehabilitation*, vol. 13, no. 1, pp. 1-14, 2016.
- [17] K. N. Gregorczyk, L. Hasselquist, J. M. Schiffman, C. K. Bensel, J. P. Obusek, and D. J. Gutekunst, "Effects of a lower-body exoskeleton device on metabolic cost and gait biomechanics during load carriage". *Ergonomics*, vol. 53, no. 10, pp. 1263-1275, 2010.
- [18] M. Hao, J. Zhang, K. Chen, H. Asada, and C. Fu, "Supernumerary robotic limbs to assist human walking with load carriage," *Journal of Mechanisms and Robotics*, vol. 12, no. 6, pp. 061014, 2020.
- [19] F. Parietti, and H. Asada, "Supernumerary robotic limbs for human body support," *IEEE Transactions on Robotics*, vol. 32, no. 2, pp. 301-311, 2016.
- [20] L. Treers, R. Lo, M. Cheung, A. Guy, J. Guggenheim, F. Parietti, and H. Asada, "Design and control of lightweight supernumerary robotic limbs for sitting/standing assistance," *In International Symposium on Experimental Robotics*, 2016, pp. 299-308.
- [21] D. J. Gonzalez, and H. Asada, "Design of extra robotic legs for augmenting human payload capabilities by exploiting singularity and torque redistribution," *In 2018 IEEE/RSJ International Conference on Intelligent Robots and Systems (IROS)*, 2018, pp. 4348-4354.
- [22] D. J. Gonzalez, and H. Asada, "Hybrid open-loop closed-loop control of coupled human–robot balance during assisted stance transition with extra robotic legs.", *IEEE Robotics and Automation Letters*, vol. 4, no. 2, pp.1676–1683, 2019.
- [23] Y. Leng, X. Lin, G. Huang, M. Hao, J. Wu, Y. Xiang, K. Zhang and C. Fu, "Wheel-legged robotic limb to assist human with load carriage: an application for environmental disinfection during COVID-19," *IEEE Robotics and Automation Letters*, vol. 6, no. 2, pp. 3695-3702, 2021.